Functional Dissection of Cdc37: Characterization of Domain Structure and Amino Acid Residues Critical for Protein Kinase Binding†

Jieya Shao, Angela Irwin, Steven D. Hartson, and Robert L. Matts*

Department of Biochemistry and Molecular Biology, Oklahoma State University, Stillwater, Oklahoma 74078-3035

Received July 1, 2003; Revised Manuscript Received September 4, 2003

ABSTRACT: Hsp90 and its co-chaperone Cdc37 facilitate the folding and activation of numerous protein kinases. In this report, we examine the structure−function relationships that regulate the interaction of Cdc37 with Hsp90 and with an Hsp90-dependent kinase, the heme-regulated eIF2α kinase (HRI). Limited proteolysis of native and recombinant Cdc37, in conjunction with MALDI-TOF mass spectrometry analysis of peptide fragments and peptide microsequencing, indicates that Cdc37 is comprised of three discrete domains. The N-terminal domain (residues 1−126) interacts with client HRI molecules. Cdc37's middle domain (residues 128−282) interacts with Hsp90, but does not bind to HRI. The C-terminal domain of Cdc37 (residues 283−378) does not bind Hsp90 or kinase, and no functions were ascribable to this domain. Functional assays did, however, suggest that residues S127−G163 of Cdc37 serve as an interdomain switch that modulates the ability of Cdc37 to sense Hsp90's conformation and thereby mediate Hsp90's regulation of Cdc37's kinase-binding activity. Additionally, scanning alanine mutagenesis identified four amino acid residues at the N-terminus of Cdc37 that are critical for high-affinity binding of Cdc37 to client HRI molecules. One mutation, Cdc37/W7A, also implicated this region as an interpreter of Hsp90's conformation. Results illuminate the specific Cdc37 motifs underlying the allosteric interactions that regulate binding of Hsp90−Cdc37 to immature kinase molecules.

The vertebrate homologue of the yeast CDC37 gene product functions as a component of the Hsp90[1] chaperone machine (reviewed in refs *1*−*3*). Cdc37 is linked to the function of a wide range of proteins, most of which belong to the eukaryotic protein kinase family. Many Hsp90-dependent kinases coexist in Hsp90−Cdc37 heterocomplexes, including the cyclin-dependent protein kinases CDK4 (*4*−*6*), CDK6 (*6*, *7*), and CDK9 (*8*, *9*); the Src family tyrosine kinases pp60v-src, Lck and Hck (*10*−*14*); casein kinase II (*15*−*17*); Raf-1 (*18*, *19*); mitogen-activated protein kinase MOK (*20*); the heme-regulated [HRI, (*13*, *21*)], the double-stranded RNA-activated [PKR, (*22*)] and the GCN2 eIF2α kinases (*23*); IκB kinase IKK (*24*); and Akt (*25*). Although Cdc37 has been dubbed the "kinase-specific cohort of Hsp90", Cdc37 has recently been found in association with the androgen receptor (*26*, *27*) and with reverse transcriptase (*28*), and both of these proteins depend on Cdc37 function for their activities. Thus, Cdc37 clients are probably not limited solely to protein kinases.

Vertebrate Cdc37 interacts directly with its partner Hsp90, thus forming a basal complex with Hsp90 in the absence of client (*13*). This basal complex is readily disrupted by high salt concentrations (*13*). Arbitrary bisection of Cdc37 indicates that the kinase-binding and Hsp90-binding activities of Cdc37 segregate to the N-terminal and C-terminal halves of the protein, respectively (*18*, *21*). Studies in our (*13*, *14*, *21*) and other labs (*5*, *18*) argue that Cdc37 is not a simple passive adaptor that tethers Hsp90 to kinases: instead, Cdc37 serves as a dynamic active chaperone partner that responds to, and mediates, Hsp90's conformational switching. In this role, Cdc37 overexpression stimulates the formation of salt-stable heterocomplexes containing Hsp90 and its client kinases, but this process is sensitive to the Hsp90 inhibitor geldanamycin, indicating that the biochemical mechanisms involve Hsp90's nucleotide-mediated conformational switching.

Few studies have investigated the structure−function relationships that modulate the interaction of Cdc37 with protein kinases and Hsp90 (*18*, *21*). Replacement of the first eight amino acids residues of Cdc37 with an arbitrary amino acid sequence eliminates binding of the mutant protein to the Hsp90-dependent HRI kinase, but does not alter binding to Hsp90 (*21*). Although Cdc37 is essential to yeast viability, a Cdc37 gene product containing residues 1−148 is sufficient

† This work was supported by the American Heart Association (0250556N), the National Institute of Health (National Institute of General Medicine GM51608 to R.L.M.), the Oklahoma Center for the Advancement of Science and Technology (HN6-018 to S.D.H.), and the Oklahoma Agricultural Experiment Station (Project 1975).

* Author for correspondence: Robert L. Matts, 246 NRC, Department of Biochemistry and Molecular Biology, Oklahoma State University, Stillwater OK 74078-3035. Tel.: (405) 744-6200. FAX: (405) 744-7799. E-mail: rmatts@biochem.okstate.edu.

[1] Abbreviations: 90-kDa heat shock protein, Hsp90; Cdc37, generically used to refer to the protein product of CDC37 gene homologues regardless of source of organism; DTT, dithiothreitol; HRI, heme-regulated eIF2α kinase; eIF, eukaryotic initiation factor; eIF2α, α-subunit of eukaryotic initiation factor 2; EDTA, ethylenediamine tetraacetic acid; IgM, immunoglobulin M; SDS−PAGE, sodium dodecyl sulfate−polyacrylamide gel electrophoresis; PIPES, piperazine-*N*,*N*′-bis[2-ethanesulfonic acid]; Harc, Hsp90-associated relative of Cdc37; DMSO, dimethyl sulfoxide; Ni^{2+}-NTA resin, Ni^{2+}-nitrilotriacetic acid coupled to agarose; PVDF; poly(vinylidene difluoride); PCR, polymerase chain reaction; RRL, rabbit reticulocyte lysate; TnT, nuclease-treated reticulocyte lysate for protein expression by coupled transcription and translation.

10.1021/bi035138j CCC: $25.00
Published on Web 10/11/2003

to support yeast viability (*29*). Recently, Scholz et al. (*30*) have proposed a domain structure for mammalian Cdc37 based on alignments of the sequence of Cdc37 with a novel mammalian Cdc37 paralogue, Harc. This alignment predicts a three-domain structure for Cdc37, with mammalian Cdc37 and Harc sharing a common middle domain (amino acids 145−264 of human Cdc37) that bears an Hsp90-binding site.

Here, we characterize the structure−function relationships that govern Cdc37's Hsp90 and kinase-binding activities. Results support a three-domain structure, with the N-terminal domain functioning to bind kinase clients and the middle domain functioning to bind Hsp90. Detailed dissections suggest that these activities are modulated by amino acid sequences that lie between Cdc37's N-terminal and central domains. Additionally, four specific N-terminal residues were identified that are critical for Cdc37's kinase-binding activity, but do not govern global Cdc37 structure, and may participate in Hsp90's regulation of Cdc37 function.

MATERIALS AND METHODS

Purification of Recombinant Cdc37 from Escherichia coli. (His_6)-Cdc37 (in pQE32 expression vector) (*21*) was overexpressed in M15[pREP4] *Escherichia coli* strain and purified following the manufacturer's recommendations. Briefly, His-tagged-Cdc37 was purified from cell lysates using Ni^{2+}-NTA affinity resin (Qiagen), washed, eluted with buffer containing 250 mM imidazole, and dialyzed against 10 mM PIPES buffer (pH 7.2) containing 150 mM NaCl.

Domain Mapping of Cdc37. Purified recombinant His-tagged-Cdc37 was mixed with various concentrations of TPCK-treated trypsin (Sigma) in 10 mM Tris-HCl buffer (pH 7.4) containing 150 mM NaCl, 4 mM $CaCl_2$, and 0.1 mM EDTA. Digestions were carried out either on ice for 6 min or at 37 °C for 30 min, and were immediately stopped by boiling in SDS sample buffer. Cdc37/enzyme ratios for trypsin digests ranged from 2000:1 (g/g) to 250:1 at 37 °C and from 200:1 to 10:1 on ice. Chymotrypsin digests were performed similarly.

To affinity-purify the N-terminal tryptic fragments of (His_6)-Cdc37, trypsinolysis reactions were stopped by adding bovine pancreas trypsin inhibitor (Sigma) at an inhibitor/trypsin ratio of 4:1 (g/g), 1% SDS, and 100 mM β-mercaptoethanol (as the final concentrations). The reaction mixture was further diluted 5 times with NaH_2PO_4 buffer (50 mM final concentration, pH 8.0) to reduce the concentrations of SDS and β-mercaptoethanol, and diluted reactions were absorbed to Ni^{2+}-NTA resin (Qiagen) for 1 h at room temperature. Adsorptions were washed 4 times with 50 mM NaH_2PO_4 buffer (pH 8.0) containing 1 M NaCl, 1% Triton X-100, and 8 M urea, were subsequently washed twice with TBS, and were then boiled in SDS−PAGE sample buffer.

Proteolytic Fingerprinting of Cdc37 in Rabbit Reticulocyte Lysates. Wild-type and mutant Cdc37 were synthesized and radiolabeled with [^{35}S]Met via coupled transcription/translation at 30 °C for 30 min, and were subsequently matured for 1 h in the presence of 60 μM aurintricarboxylic acid to inhibit reinitiation of protein synthesis. Reactions were then chilled on ice and treated with TPCK-treated trypsin for 6 min. Digestions were terminated by addition of SDS−PAGE sample buffer and immediate boiling, after which they were separated by SDS−PAGE and analyzed by autoradiography.

Identification of Cdc37 Domains. To identify the peptides representing each product produced by Cdc37 nicking assays, gel pieces containing the major proteolytic-nicking fragments were analyzed by standard proteomics fingerprinting techniques. Briefly, each band was excised from the polyacrylamide gel, washed, reduced with DTT, and alkylated with iodoacetamide. After additional washing of the sample, dehydrated gel pieces were infiltrated with trypsin (Promega, sequencing grade), digested overnight, and the digested peptides were extracted and analyzed by MALDI-TOF mass spectrometry. Mass characterizations were performed using α-cyano-4-hydroxycinnamic acid as matrix, and spectra were acquired in both linear and reflector modes using external standards as calibrants. In instances in which contiguous peptides representing domain junctions were not observed, Edman sequencing was used to identify the N-terminus of each individual protein band representing a product from nicking proteolysis.

Construction of Plasmids Encoding Cdc37 Domains. PCR fragments were generated using oligonucleotide primers corresponding to the border region identified for each domain of human Cdc37, as previously described (*31*−*33*). PCR products were ligated into the expression vectors pSP64T (*34*) and derivatives thereof, and constructs were verified by DNA sequencing. To facilitate cloning, domain constructs D2 and D12 were terminated at E282 and D3 was constructed to contain R283.

Site-Directed Mutagenesis of Cdc37. Point mutations at the N-terminus of Cdc37 were introduced using standard PCR-based methodologies. Mutagenesis utilized seven oligonucleotides (upper primers) corresponding to the N-terminus of human Cdc37 and encoding the desired X → A mutation, as well as complementary sense coding sequence and upstream restriction sites for subcloning. PCR products were ligated into a modified pSP64T vector (*13*), and the fidelity and efficacy of each mutation were subsequently confirmed by DNA sequencing.

Immunoadsorptions from Rabbit Reticulocyte Lysate. Polypeptides representing truncated Cdc37 constructs with an N-terminal His-tag were synthesized and radiolabeled with [^{35}S]Met via coupled transcription/translation in nuclease-treated rabbit reticulocyte lysate for 30 min at 30 °C, followed by a 10 min chase with the addition of protein synthesis initiation inhibitor aurintricarboxylic acid (60 μM). Cdc37 gene products were either directly immunoabsorbed with agarose-bound anti-(His_5) antibody (Qiagen), or with monoclonal anti-Hsp90 antibody 8D3 (*35*). Adsorptions were then assessed by Western blotting and/or autoradiography. To examine kinase-binding activities of each Cdc37 gene product, non-His-tagged versions of the domains were mixed with reticulocyte lysate containing newly synthesized [^{35}S]-labeled His-tagged HRI and were subsequently coadsorbed with anti-His antibody. Immunoresins were washed 4 times with 10 mM PIPES buffer (pH 7.2) containing 150 mM NaCl and 0.5% Tween-20, and coadsorption of [^{35}S]-labeled gene products was analyzed by SDS−PAGE and autoradiography.

RESULTS

Domain Mapping of Cdc37. Although early studies had ascribed segregating functions to arbitrarily bisected Cdc37 gene products, this bisection provided little insight into

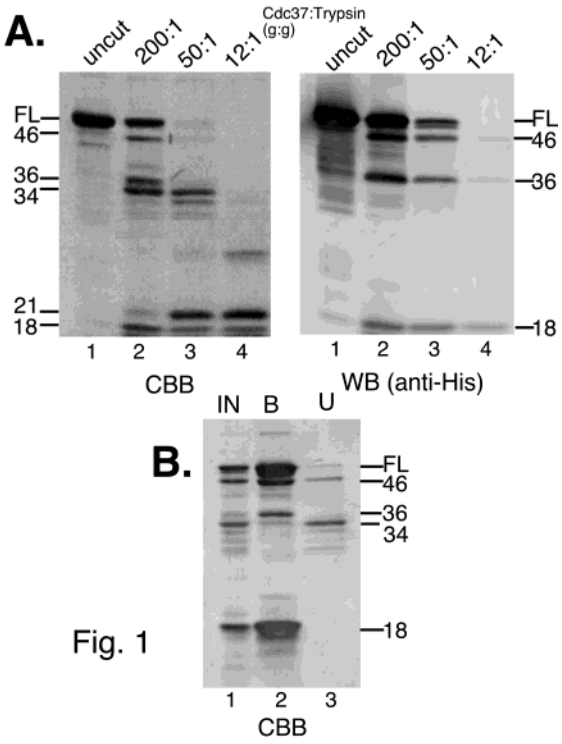

Fig. 1

FIGURE 1: Limited trypsinolysis of purified recombinant His-tagged-Cdc37. (A) 5 μg of purified recombinant His-tagged-Cdc37 was digested with trypsin at substrate/enzyme ratios of 200:1 (lane 2), 50:1 (lane 3), and 12:1 (lane 4), respectively, as described under Materials and Methods. A mock digestion containing equal amount of trypsin-free buffer was set up in parallel as the uncut control (lane 1). Digestion was carried out for 6 min on ice and stopped immediately by mixing with boiling SDS sample buffer. Proteolytic fragments were subsequently separated on a 12% SDS−polyacrylamide gel, transferred to PVDF membrane, and stained with Coomassie brilliant blue R250 (CBB, left panel). After imaging, the membrane was bleached with methanol to remove the dye and immunoblotted with the anti-His-tag antibody (WB, right panel). (B) 10 μg of purified recombinant His-tagged-Cdc37 was digested with trypsin at a substrate/enzyme ratio of 200:1 for 6 min on ice. Digestion was terminated by mixing with the trypsin inhibitor along with SDS and β-mercaptoethanol at concentrations as described under Materials and Methods. Samples were absorbed to Ni^{2+}-NTA resin, and both the bound (B: lane 2) and unbound (U: lane 3) Cdc37 fragments were analyzed by SDS−PAGE, transferred to PVDF membrane, and stained with Coomassie Brilliant Blue R250 (CBB) as described under Materials and Methods. IN: aliquot of unfactionated cleaved Cdc37. FL: full-length His-tagged Cdc37, with numbers below indicating the estimated molecular weight of bands in kDa.

Cdc37's true domain architecture. Thus, we utilize limited proteolytic digestion of native Cdc37 molecules to identify flexible protease-accessible regions that might represent interdomain regions. As shown in Figure 1A, a Cdc37/trypsin ratio of 200:1 generated four major proteolytic fragments with M_r's of approximately 46 000, 36 000, 34 000, and 18 000. Some minor fragments were also apparent, but were not further characterized. At higher trypsin concentrations, a fragment with an M_r of 21 000 was apparent, and this fragment remained intact under all trypsin concentrations utilized. The high protease-resistance of this particular fragment indicated that its tertiary structure was highly protease resistant, suggesting the compact solvent inaccessible structure typical of authentic protein domains.

To interpret Cdc37's limited-proteolysis map, the proteolytic fragments were transferred to PVDF and immunoblotted with antibody directed against the N-terminal His-epitope tag. Blotting indicated that the 46 000, 36 000, and 18 000 M_r fragments contained the N-terminus, whereas the 34 000 M_r fragment and the highly protease-resistant 21 000 M_r fragment lacked this tag, i.e., were either internal or C-terminal fragments [Figure 1A: WB (anti-His)]. To confirm this observation, Cdc37 was digested at the optimal 200:1 ratio, and the mixture of tryptic fragments were affinity purified on Ni^{2+}-NTA affinity resin under denaturing conditions. Consistent with the results from Western blotting, the 46 000, 36 000, and 18 000 M_r fragments were specifically adsorbed by the resin, whereas the 34 000 M_r fragment was not (Figure 1B).

Table 1: Mass Spectrometry Analysis of Major Proteolytic Fragments of Cdc37

Major Cdc37 fragments	Measured mass (Da)	Calculated mass (Da)	Covered sequences
46 kDa / 36 kDa / 18 kDa	810.28	810.38	M40EQFQK45
	1529.49[a]	1529.78[a]	E70LEVAEGGKAELER83
	1056.49	1056.58	L84QAEAQQLR92
	1335.43[a]	1335.64[a]	S97WEQKLEEMR106
	1811.71[a]	1811.86[a]	S111MPWNVDTLSK DGFSK126
46 kDa / 34 kDa / 21 kDa	2493.69[a]	2493.18[a]	S127MVNTKPEKTEEDSEEVREQK147
	1043.60[a]	1043.54[a]	T150FVEKYEK157
	760.27	760.39	H161FGMLR166
	934.13[a]	934.44[a]	R167 WDDSQK173
	1672.44[a]	1671.84[a]	V228DPRACFRQFFTK240
	1721.45[a]	1720.75[a]	Q247YMEGFNDELEAFKER262
	658.34[a]	658.43[a]	L269RIEK273
	1313.42[a]	1313.57[a]	A274MKEYEEEER283
46 kDa / 34 kDa	2269.62	2269.16	L287GPGGLDPVEVYESLPEELQK307
	2006.09[a]	2005.96[a]	D313VQMLQDAISKMDPTDAK330
	734.16	734.34	Y331HMQR335
	1707.65	1707.84	E353GEEAGPGDPLLEAVPK369

[a] Peptides resulting from partial trypsin digestion.

Characterizations of the Major Proteolytic Fragments of Cdc37. To identify the N- and C-termini of each Cdc37 fragment/domain, each fragment was excised from SDS−PAGE gels and subjected to exhaustive digestion with trypsin. Peptides produced from this exhaustive digestion were sized by mass spectrometry, and their identities were determined by comparison of experimental peptide masses with the masses of Cdc37's theoretical trypsinolysis products (Table 1).

The first Cdc37 interdomain junction was identified on the basis of two peptides from a contiguous stretch of Cdc37, namely, the peptides with *m*/*z*'s of 1811 and 2493, which represented the sequences S111-to-K126 and S127-to-K147, respectively (Table 1). These peptides contained abutting termini, and both were readily detected. Thus, the presence or absence of these peptides in the exhaustive proteolytic digests of Cdc37 fragments generated by limited nicking proteolysis were unambiguous identifiers of each fragment's termini. These characterizations unambiguously identified the

region immediately surrounding K126 as a major region of flexibility in full-length folded Cdc37 molecules. Consistent with this conclusion, Edman sequencing yielded (S−M−V−N−T−K−P−E) as the N-terminal sequence of the 21 kDa fragment.

The second major region generated from limited nicking proteolysis of Cdc37 was similarly identified. Two peptides representing Cdc37 amino acid sequences from A274 to R283 and L287 to K307 were readily detected, and the presence or absence of these peptides in the products generated from proteolytic digestion of Cdc37 fragments were unambiguous identifiers of these products' termini. However, R283 is immediately followed by the sequence KKR, all of which represent potential trysin cleavage sites. Thus, while the exact site of trypsinolytic cleavage could not be identified, these data nonetheless identify the region from R283 to L287 as a major area of flexibility in full-length folded Cdc37 molecules.

In contrast to those proteolytic nicking products whose C-termini could be mapped on the basis of the absence of readily detectable peptides, the C-termini of the 46 000 M_r and 34 000 M_r fragments were inferred. The peptide products of exhaustive digestion of the 34 000 M_r fragment lacked detectable peptides beyond K369. However, the sequence of this C-terminal region predicts two very short peptides whose detection was obscured by low-mass noise inherent to MALDI ionization and the matrix used for the same. Therefore, it remains unclear whether the 34 000 M_r fragment contains the last nine amino acids of Cdc37 or not.

Analysis of the 46 000 M_r fragment assigned it to residues 1−335 or 1−352. The absence of the readily detectable peptide that spans residues 353−369 and the presence of the peptide that terminates at 335 indicate that the 46 000 M_r fragment is generated by cleavage at one of three sites predicted from the Cdc37 sequence versus trypsin's known cut specificity: R335, K347, or K352. However, since this region is very close to the C-terminus of Cdc37 (378), it is probably not a true interdomain junction. Instead, it may a flexible region that separates the last 25−30 amino acids of Cdc37 from the major part of its C-terminal domain.

Thus, limited proteolysis of the native full-length Cdc37 gene product, Western blotting and affinity chromatography for the N-terminal epitope tag, and exhaustive trypsinolysis/MALDI-TOF MS characterizations of proteolytic fragments produced a detailed and internally consistent map of Cdc37's putative domain structure (Figure 2). Furthermore, this map was consistent with previously proposed interdomain regions predicted from aligning Cdc37 with its paralogue Harc (*30*).

Characterizations of the Interactions of Cdc37 Domain Constructs with Hsp90. Early studies had assigned the kinase- and Hsp90-binding sites of Cdc37 to the arbitrary N-terminal (Cdc37/ΔC, M1-G163) and C-terminal (Cdc37/ΔN, M164-V378) halves of this protein, respectively (*18*, *21*). Thus, this previous work with the arbitrary bisections, in conjunction with sequence alignments indicating that the central region of Cdc37 and Harc have high sequence similarity (*30*) and with our mapping presented above, predicted that the middle domain D2 would bear the Hsp90-binding function of Cdc37. To characterize this function, His-tagged Cdc37 gene products (diagrammed in Figure 2B) representing each of the three putative domains of Cdc37 were synthesized and concomitantly radiolabeled in reticulocyte lysates containing active endogenous Hsp90. Additionally, two His-tagged constructs representing contiguous neighboring domains, named D12 (M1−E282) and D23 (M164−V378), were also synthesized. Subsequently, the Hsp90-binding activities of each domain were assessed through immunoadsorption of the Cdc37 gene products and Western blotting for concomitant binding of Hsp90. Full-length Cdc37, as well as the two arbitrary domains, Cdc37/ΔC and Cdc37/ΔN, were also synthesized to serve as controls and benchmarks from previous characterizations (*18*, *21*).

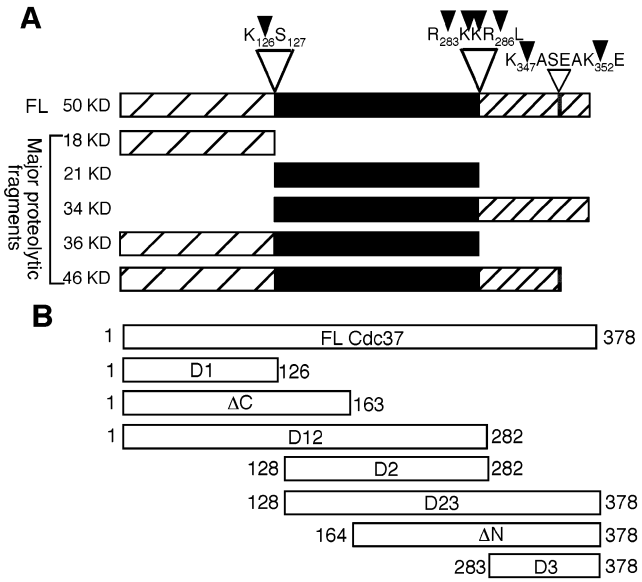

FIGURE 2: Domain structure of Cdc37. (A) Mapping of the major proteolytic fragments of Cdc37 resulting from limited trypsinolysis by MALDI-TOF. Two major trypsin cutting sites representing putative interdomain junctions are shown by large arrows pointing to the exact or approximate locations. One minor cutting site possibly representing an intradomain junction is shown by a small arrow. Major proteolytic fragments of Cdc37 are also shown according to their individual locations. (B) Dissection of Cdc37 based on its domain structure (shown in A). D1, D2, and D3 are the putative individual domains whereas D12 and D23 are fusions of adjacent domains. The arbitrary domains Cdc37/ΔC and Cdc37/ΔN, which have been characterized previously are also shown here. Note D2 and D23 lack S127, as they were constructed to start with M128 in the Cdc37 sequence.

As previously demonstrated (*21*), Western blotting for the coadsorption of Hsp90 indicated that full-length Cdc37 and Cdc37/ΔN specifically interacted with Hsp90 (Figure 3). In agreement with our predictions, the central domain D2 bound to Hsp90, whereas the other two domains D1 and D3 did not. Also as predicted, D12 and D23, which both contained the central domain D2, also specifically pulled down endogenous Hsp90. D2 and D23 had slightly reduced Hsp90 binding activity, while the interaction of Cdc37/ΔN with Hsp90 was significantly decreased compared to full-length Cdc37 or the D12 construct. Quantification of the amount of construct expressed and normalization to the methionine content of each Cdc37 gene product indicated that the reduced binding of Cdc37/ΔN to Hsp90 relative to the binding of wild-type Cdc37 (65−75%) was significant. Thus, the Hsp90-binding site was confirmed to be located in the central domain D2 of Cdc37.

The basal interaction of wild-type Cdc37 with Hsp90 is not dramatically affected by the Hsp90 inhibitor geledanamycin (*13*, *21*). Thus, we examined whether geldanamycin-

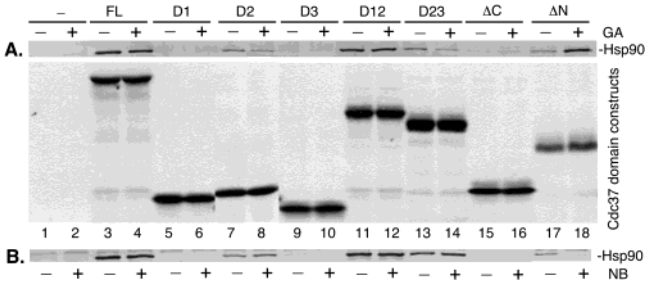

FIGURE 3: Hsp90-binding activities of Cdc37 dissection products. (A) Eight different [^{35}S]-labeled His-tagged Cdc37 constructs (full-length, D1, D2, D3, D12, D23, Cdc37/ΔC, and Cdc37/ΔN) were synthesized in TnT RRL containing (GA: even-number lanes, (+) or lacking (DMSO, vehicle control: odd-number lanes, (−) 10 μg/mL geldanamycin (GA: +) at 30 °C for 30 min followed by 10 min chase upon the addition of 60 μM aurintricarboxylic acid. (B) After radiolabeling Cdc37 constructs as described above (no additions), 2 mM novobiocin (NB: +, even numbered lanes) or an equivalent volume of 10 mM Tris-HCl, pH 8.0 (odd numbered lanes: (−) was subsequently added, and the samples were incubated for an additional 25 min. Two mock RRL reactions lacking the exogenous DNA templates were assessed in parallel as the controls for nonspecific binding (lanes 1 and 2) in each experiment. All the reactions were subsequently immunoprecipitated by the anti-His-tag antibody and separated on a 10% SDS−polyacrylamide gel. Proteins were then transferred to PVDF membrane, and analyzed by autoradiography (A: lower panel) for immunoadsorbed [^{35}S]-labeled Cdc37 domain constructs or Western blotting (A: upper panel; and B) for coadsorbed endogenous Hsp90, respectively. The autoradiogram for the [^{35}S]-labeled Cdc37 domain constructs in the experiment examining the effect of novobiocin is not shown, as it was essentially the same as that shown in panel A, except that little, if any, immunoadsorbed [^{35}S]-labeled His-tagged Cdc37/ΔN was detectable in the lane comparable to lane 18 of the data shown (see Figure 4).

induced alterations in Hsp90's conformations might alter its interaction with truncated Cdc37 constructs. Assessment of Hsp90 binding to each of the truncated Cdc37 gene products (Figure 3) demonstrated that geldanamycin had a modest effect on the interaction between Hsp90 and D2 or D23 (Figure 3). Geldanamycin had no effect on the interactions of Hsp90 with full-length Cdc37 or D12. As expected, Hsp90 did not bind to the D1, D3, or Cdc37/ΔC constructs in the presence of geldanamycin. Quite surprisingly, however, the interaction between Hsp90 and the Cdc37/ΔN was enhanced severalfold by GA treatment to a level equivalent to the binding of full-length Cdc37 to Hsp90 (Figure 3, lane 18).

Cdc37 function is modulated by Hsp90's nucleotide-dependent conformational switching, and Cdc37 binding to client kinases is inhibited by geldanamycin-induced inhibition of Hsp90 (*13*, *21*). The observation that the basal interaction of Cdc37/ΔN with Hsp90 was decreased by 65−75% (relative to full-length Cdc37), and that application of geldanamycin restored the binding of Cdc37/ΔN to Hsp90 to that of the full-length Cdc37 gene product (Figure 3) was quite surprising, as this does not reflect the normal effect of this compound on the interaction of Hsp90 with Cdc37 [(*13*, *21*) and Figure 3, lanes 3 and 4]. This difference between the effects of geldanamycin on Hsp90's affinity for full-length Cdc37 versus Cdc37/ΔN are consistent with previous demonstrations that geldanamycin generates or enforces specific Hsp90 conformations (*13*, *36*). However, this result also provides strong evidence for the novel observation that in unfractionated native cell lysates [i.e., not "salt-stripped" (*36*)], the basal conformation of Hsp90 is not equivalent to

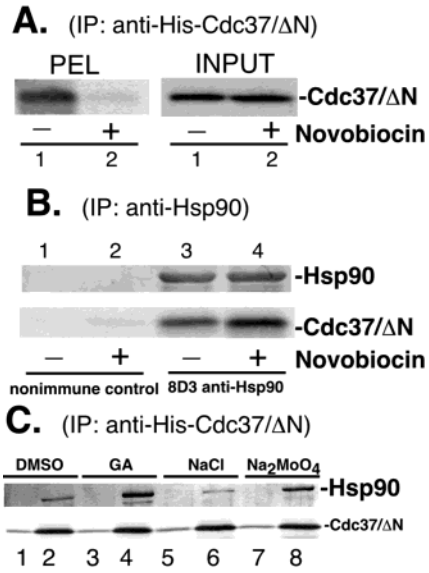

FIGURE 4: Effect of novobiocin on the interaction of Cdc37/ΔN with Hsp90. [^{35}S]His-tagged Cdc37/ΔN was synthesized in TnT RRL for 25 min at 30 °C, followed by a 10 min chase with the addition of 60 μM aurintricarboxylic acid. (A) Novobiocin (2 mM: lane 2) or an equivalent volume of 10 mM Tris-HCl, pH 8.0 (lane 1, vehicle control), or (C) DMSO (vehicle control, lanes 1 and 2), 10 μg/mL geldanamycin (GA, lanes 3 and 4), 50 mM NaCl (NaCl, lanes 5 and 6) or 20 mM sodium molybdate (Na_2MoO_4, lanes 7 and 8) were subsequently added. The samples were incubated for 25 min, and then immunoadsorbed to anti-His-tag antibody resin (A, PEL or C: lanes 2, 4, 6, and 8) or nonimune control antibody (C: lanes 1, 3, 5, and 7). Aliquots of lysate containing [^{35}S]His-tagged Cdc37/ΔN were taken prior to immunoprecipitation (A, INPUT). Samples were analyzed by SDS−PAGE and autoradiography (A and C: Cdc37/ΔN) or Western blotting (C: Hsp90). (B) [^{35}S]His-tagged Cdc37/ΔN was synthesized in TnT RRL and incubated with or without novobiocin as described above, and subsequently immunoadsorbed with 8D3 anti-Hsp90 monoclonal antibody (8D3 anti-Hsp90) or nonimmune mouse IgM antibody (nonimmune control). Samples were separated on SDS−PAGE and visualized by autoradiography, Cdc37/ΔN or Coomassie blue staining, Hsp90.

the geldanmycin-bound conformation of Hsp90. In addition to providing evidence for an altered Hsp90 conformation, geldanamycin's stimulation of Hsp90's binding to Cdc37/ΔN indicates the Cdc37/ΔN can perceive Hsp90's conformation, and that additional Cdc37 segments deleted from this construct (i.e., the N-terminal half of Cdc37's Hsp90-binding domain, the interdomain region and/or the kinase-binding domain) normally modulate this recognition.

To further investigate the hypothesis that Cdc37/ΔN can perceive Hsp90's conformation, the effect of the Hsp90 inhibitor novobiocin on the interaction of Cdc37/ΔN with Hsp90 was investigated. Novobiocin binds to a second nucleotide-binding site located in the central/C-terminal region of Hsp90 (*37*−*39*). The binding of full-length Cdc37, D2, D12, and D23 to Hsp90 was not affected by the presence of novobiocin, while little, if any, Hsp90 was coadsorbed with His-tagged Cdc37/ΔN (Figure 3B). However, the absence of coadsorbed Hsp90 correlated with absence of immunoadsorbed [^{35}S]-labeled His-tagged Cdc37/ΔN (see Figure 4).

To investigate this observation further reciprocal immunoprecipitations were carried out to compare the ability of anti-His-tag antibodies to coadsorb Hsp90 with His-tagged Cdc37/

ΔN versus the ability of anti-Hsp90 antibodies to coadsorb Cdc37/ΔN. In the presence of novobiocin, the ability of anti-His-tag antibodies to immunoadsorb His-tagged [^{35}S]Cdc37/ΔN, (and to thus coadsorb Hsp90) was markedly impaired (Figure 4). However, direct immunoadsorption of Hsp90 demonstrated that novobiocin did not inhibit the interaction of Cdc37/ΔN with Hsp90: in fact, a slight increase in binding was observed (Figure 4). This surprising result suggested that novobiocin generated an Hsp90 conformation that somehow led to the masking of the N-terminal segments of Cdc37/ΔN from recognition by the anti-His antibody. The novobiocin-induced conformation of Hsp90 was also not equivalent to that induced by the binding of molybdate to Hsp90, as the presence of molybdate like geldanamycin enhanced the amount of Hsp90 that coadsorbed with His-tagged Cdc37/ΔN compared to the control, and did not affect the ability of the anti-His-tag antibody to interact with Cdc37/ΔN bound to Hsp90 (Figure 4C). In toto, these data indicate that three conformations of Hsp90 can be distinguished through the effects of Hsp90-binding drugs, and that Cdc37's ability to differentiate these conformations resides in amino acids M164−V378 of Cdc37. The observation that the interaction between Hsp90 and Cdc37 constructs that contain amino acid residues S127−G163 are not similarly affected by geldanamycin or novobiocin suggests that this region may be involved in negatively modulating Cdc37's ability to respond to or sense conformations of Hsp90 induced by nucleotide mediated switching.

Characterizations of the Interactions of Cdc37 Domain Constructs with Kinase. Previous observations that Cdc37's kinase-binding activity segregates to its N-terminal region, and the finding that D2 binds Hsp90, suggested that D1 represents Cdc37's kinase-binding domain. To test this hypothesis, [^{35}S]labeled truncated Cdc37 gene products representing individual or tandem Cdc37 domains were synthesized in reticulocyte lysate. These reaction mixtures were subsequently mixed with reticulocyte lysate reactions containing newly synthesized His-tagged-HRI, wherein hemin concentrations were sufficient to prevent HRI maturation/activation to an Hsp90-independent state (*32*). After mixing of the sample, His-tagged HRI was immunoadsorbed with anti-His-tag antibodies, and the coadsorption of [^{35}S]-labeled Cdc37 gene products was assessed by autoradiography. Consistent with our hypothesis, both D1 and D12 were specifically coadsorbed by His-tagged HRI (Figure 5A: PEL), indicating that D1 (amino acids M1−K126) contained Cdc37's kinase-binding site. In contrast, very little D23 (residues M128−V378) and no D2 (residues M128−E282) were specifically coadsorbed with HRI in the absence (Figure 5B, PEL: D2 and PEL: D23) or presence (not shown) of geldanamycin.

Previously, we demonstrated that Cdc37 binds to HRI in an Hsp90-dependent manner, and that this interaction is fully disrupted by geldanamycin (*13*, *21*). In contrast, the interaction between the Cdc37/ΔC construct and HRI had been found to be GA-insensitive, presumably because in the absence of the C-terminal Hsp90-binding domain, the kinase-binding site is no longer regulated by nucleotide-modulated conformational switching of Hsp90 [(*18*, *21*) and Figure 6B, lane 4]. Thus, we predicted that the interaction of D1 with HRI would similarly not be sensitive to disruption by geldanamycin, whereas D12 would behave the same as the

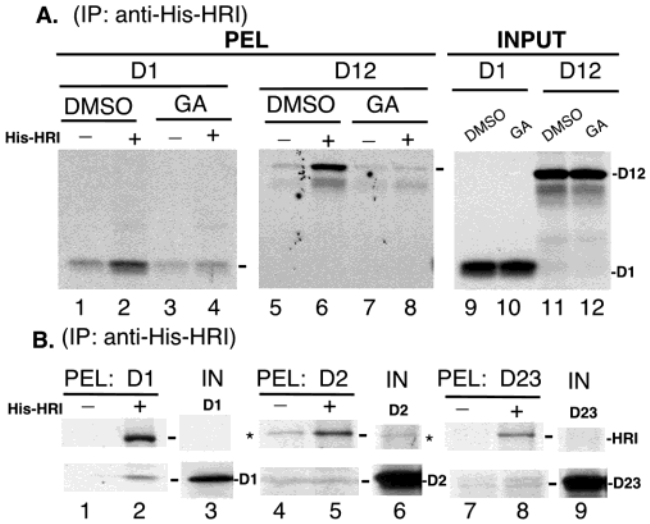

FIGURE 5: HRI-binding activities of of Cdc37 domain constructs. [^{35}S]-Labeled D1 or D12 were synthesized in TnT rabbit reticulocyte containing (lanes 3, 4, 7, and 8) or lacking (lanes 1, 2, 5, and 6) 10 μg/mL geldanamycin (GA) at 30 °C for 30 min. After a 10 min chase with 60 μM aurintricarboxylic acid, the reaction mixtures were mixed with either mock reticulocyte lysate (−: lanes 1, 3, 5, and 7) or TnT lysate containing newly synthesized His-tagged-HRI (+: lanes 2, 4, 6, and 8) and further incubated for 25 min at 30 °C. The samples were then subjected to immunoadsorption using the anti-His-tag antibody and analyzed SDS−PAGE on a 10% gel, transferred to PVDF membrane, and the coadsorbed [^{35}S]-labeled D1 (PEL, left panel) and D12 (PEL, right panel) were visualized by autoradiography analysis. Aliquots of RRL mixtures were taken prior to immunoadsorption and analyzed to show that geldanamycin had no effect on the synthesis level of D1 and D12 (INPUT). (B) [^{35}S]-Labeled D1, D2, or D23 were synthesized in TnT RRL (no additions), and mixed and incubated with either mock reticulocyte lysate (−: lanes 1, 4, and 7) or TnT RRL containing newly synthesized His-tagged HRI (+: lanes 2, 5, and 8) as described above. The samples were then subjected to immunoadsorption using the anti-His-tag antibody and analyzed as described above. Coadsorbed [^{35}S]-labeled D1 (lanes 1 and 2), D2 (lanes 4 and 5) and D23 (lanes 7 and 8) were visualized by autoradiography. PEL: D1, PEL: D2, and PEL: D3. Panels showing portions of the autoradiogram containing immunoadsorbed HRI and any coadsorbed [^{35}S]-labeled D1, D2, or D23. IN, Panels from the autoradiogram of aliquots of unfractionated TnT lysate containing [^{35}S]labeled D1, D2, and D23 prior to mixing with RRL containing His-HRI RRLor mock RRL showing the areas of autoradiogram containing labeled Cdc37 domains and the area where HRI migrates. Note (*) marks the mobility of a [^{35}S]-labeled band present in the D2 translation (D2/IN), that has a mobility similar to HRI and nonspecifically binds to the anti-His tag resin.

full-length Cdc37 because of the presence of Cdc37's Hsp90 binding domain. Surprisingly, however, while geldanamycin disrupted the interaction between D12 and HRI, geldanamycin also disrupted the interaction between D1 and HRI (Figure 5A). Thus, the kinase-binding activity of D1, which lacks residues S127-G163 and other known Hsp90-binding segments, was somehow dependent upon Hsp90's nucleotide modulated conformational switching, and differed substantially from the kinase-binding activity previous described for the Cdc37/ΔC construct containing the S127−G163 Cdc37 segment.

Bisection of Cdc37 Uncouples Cdc37's Hsp90-Binding Activity from Its Kinase-Binding Activity. Previous work has demonstrated that full-length Cdc37 is not recruited to Hsp90−kinase complexes formed in the presence of geldanamycin (*13*, *21*). Thus, the ability of Cdc37 to form stable

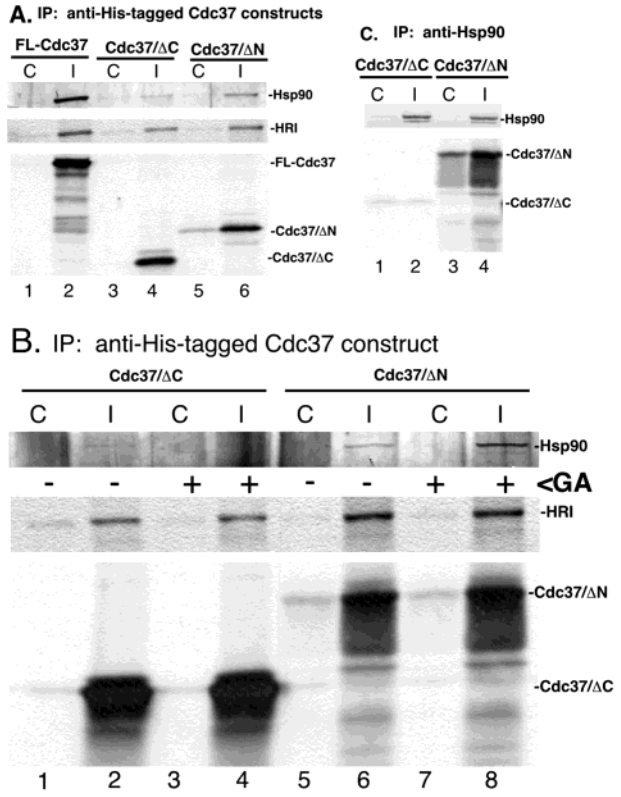

FIGURE 6: Bisection of Cdc37 uncouples Hsp90-binding activity from Cdc37's kinase-binding activity. (A) [^{35}S]-Labeled HRI was synthesized in TnT RRL, and mixed and incubated for 20 min with TnT RRL containing [^{35}S]-labeled His-tagged full-length Cdc37 (lanes 1 and 2), Cdc37/ΔC (lanes 3 and 4), or Cdc37/ΔN (lanes 5 and 6) as described in Figure 5. Samples were immunoadsorbed to anti-His-tag antibody (I) or nonimmune antibody resin (C) and analyzed as described in Figure 5. [^{35}S]-His-tagged Cdc37 constructs (lower panel), and coadsorbed [^{35}S]-HRI (middle panel), and Hsp90 (upper panel) were visualized by autoradiography and Western blotting, respectively. (B) [^{35}S]-Labeled HRI that was synthesized in TnT RRL in the presence (lanes 3, 4, 7, and 8) or absence (lanes 1, 2, 5, and 6) of 10 μg/mL geldanamycin, and mixed, TnT RRL containing [^{35}S]-labeled His-tagged Cdc37/ΔC (lanes 1−4), or Cdc37/ΔN (lanes 5−8) as described in Figure 5. Samples were immunoadsorbed to anti-His-tag antibody (I) or nonimune control antibody (C) resin and analyzed as described above. Coadsorption of Hsp90 (upper panel), and [^{35}S]-HRI (middle panel), and [^{35}S]-His-tagged Cdc37 construct (lower panel) were analyzed by Western blotting and autoradiography, respectively. (C) [^{35}S]-Labeled His-tagged Cdc37/ΔC (lanes 1 and 2), or Cdc37/ΔN (lanes 3 and 4) were synthesized in TnT RRL for 30 min at 30 °C. Samples were immunoadsorbed to anti-Hsp90 antibody (I) or nonimune control antibody (C) resin and analyzed as described above. Hsp90 (upper panel) and coadsorbed [^{35}S]-Cdc37 constructs (lower panel) were detected by Western blotting and autoradiography, respectively.

ternary complexes with Hsp90−kinase complexes requires the ability of Hsp90 to undergo an ATP-mediated conformation change (*13*, *21*). Results presented above indicated that while Cdc37/ΔN, which lacks D2 residues M128−G163, binds to Hsp90 (Figure 3), and can differentiate the "default" Hsp90 conformation from Hsp90 conformations induced by geldanamycin or novobiocin (Figures 3 and 4), D2 and D23 do not similarly differentiate between these conformations of Hsp90. Thus, conformational sensing appeared to be mediated by the C-terminal half of D2 (M164−E282), but was dampened by the N-terminal half of this domain (D2 residues M128−G163).

To determine whether residues M128−G163 may play a similar role in dampening the interaction of Cdc37 with Hsp90−kinase, we examined the ability of the Cdc37/ΔN to coadsorb both Hsp90 and kinase. Cdc37, Cdc37/ΔC, and Cdc37/ΔN were expressed and subsequently mixed with reticulocyte lysate containing newly synthesized molecules of the Hsp90−Cdc37 client [^{35}S]HRI. As previously observed, [^{35}S]HRI was coadsorbed with His-tagged Cdc37 and Cdc37/ΔC (Figure 6A). While Hsp90 was coadsorbed with full-length Cdc37, only a trace of Hsp90 was observed to coadsorb with Cdc37/ΔC. Under more stringent washing conditions, no Hsp90 was observed to coadsorb with Cdc37/ΔC (Figure 6B and Figure 3, lanes 15 and 16). [^{35}S]HRI and Hsp90 were also observed to coadsorb with His-tagged Cdc37/ΔN (Figure 6A,B). We next examined the effect of geldanamycin on the interaction of His-tagged HRI with His-tagged Cdc37/ΔC and Cdc37/ΔN. As previously described (*21*), Cdc37/ΔC coadsorbed HRI, Hsp90 was absent from these complexes, and this interaction was unaffected by geldanamycin (Figure 6B). In contrast, Hsp90 and HRI were coadsorbed with His-tagged Cdc37/ΔN. As observed in Figure 3, geldanamycin markedly increased the amount of Hsp90 that was coadsorbed with His-tagged Cdc37/ΔN (Figure 6B, lane 8 versus 6). Anti-Hsp90 immunoadsorptions coadsorbed Cdc37/ΔN, but not Cdc37/ΔC, confirming that Cdc37/ΔN directly interacts with Hsp90 in the absence of kinase client (Figure 6C). Thus, the presence of Cdc37/ΔN in complexes formed between Hsp90 and kinase is most probably due to its ability to bind Hsp90.

Characterization of N-Terminal Residues of Cdc37 that Are Essential for its Interaction with HRI. Sequence alignments of Cdc37 homologues from different species indicate that the first 30 or so amino acids are the most highly conserved region, suggesting that they are functionally essential [Figure 7 and (*4*, *5*)]. This alignment was consistent with our previous demonstration that replacement of the first eight amino acids of Cdc37 with a short arbitrary sequence inhibits the ability of the mutant Cdc37 construct to bind kinase, but not Hsp90 (*21*).

To examine the function of the first seven amino acids in more detail, amino acids 2−8 of Cdc37 were individually mutated to alanine, and the resulting mutants were assayed for the ability to bind kinase (HRI) and Hsp90. Non-His-tagged constructs of the Cdc37-alanine mutants were synthesized and labeled with [^{35}S]Met in reticulocyte lysate, and were subsequently mixed with reticulocyte lysate containing newly synthesized [^{35}S]His-tagged-HRI. HRI heterocomplexes were immunoadsorbed with anti-His-tag antibody, and the coadsorption of [^{35}S]-labeled Cdc37 mutants was analyzed by autoradiography.

The kinase-binding activities of V2A, D3A, Y4A, and W7A were inhibited by 65, 90, 100, and 100%, respectively (Figure 8). These results indicated that V2, D3, Y4, and W7 were important for either the interaction of Cdc37 with the kinase or for maintaining the structure of Cdc37's kinase-binding domain. Conversely, mutation of S5, V6, and D8 had no effect on the ability of Cdc37 to bind HRI, indicating that they do not play a critical role in kinase-binding by Cdc37 nor maintenance of Cdc37's secondary/tertiary structures. These findings were further consistent with the fact that D1 domain contains Cdc37's kinase-binding site.

```
Animal              :*** *. **:*****  :******..*********:***     :  .:.
Homo             --MVDYSVWDHIEVSDDED-ETHPNIDTASLFRWRHQARVERMEQFQKEKEELDRGCREC 57
Mus              --MVDYSVWDHIEVSDDED-ETHPNIDTASLFRWRHQARVERMEQFQKEKEELDRGCREC 57
Gallus           --MVDYSVWDHIEVSDDED-ETHPNIDTASLFRWRHQARVERMEQFQKEKEELDKGCREC 57
Xenopus          --MVDYSVWDHIEVSDDED-DTHPNIDTASLFRWRHQARVERMEEFDKEKEELSKAANDS 57
Silurana         --MVDYSVWDHIEVSDDED-DTHPNIDTASLFRWRHQARVERMEQFDKEKEELSKGTSDC 57
Tetraodon        MSRIDYSVWDHIEVSDDED-VSHPNIDTPSLFRWRHQARVERMEDFKKKGDDLNKGLQEC 59
Danio            MTTIDYSVWDHIEVSDDED-DTHPNIDTPSLFRWRHQARVERMEAFTQKGVELEKSLMES 59
Drosophila       --MVDYSKWKNIEISDDED-DTHPNIDTPSLFRWRHQARVERMAEMDHEKDELKKKRQSY 57
Amblyomma        --MVDYSKWKTIEVSDDED-DTHPNIDTPSLFRWRHQARVERMNELKKEREEFNKKKAKN 57
Arcoptes         --MVDYSKWKNIEISDDED-DTHPNIDTAGLFRWRHQARVERMEGQRKEKEEFEMKKKEN 57
Caenorhabditis    MPIDYSKWKDIEVSDDED-DTHPNIDTPSLFRWRHQARLERMAEKKMEQEKIDKEKGTT 58

Fungal            * :****** :*:*****:********:***: :*..** :*  *. .:        :
Metarhizium      -MPVDYSKWDALELSDDSDIEVHPNVDKRSFIRAKQNQIHQERQQRKLQIEAYKYERLIH 59
Neurospora       -MPVDYSKWDALELSDDSDVEVHPNVDKRSFIRAKQNQIHAERQQRKLQIETLKYERIIN 59
Magnaporthe      -MPLDYSKWDALELSDDSDIEVHPNVDKRSFIRAKQNQIHMERAQRKQQIETLKYERIVN 59
Paracoccid.      -MVLDYSKWDALELSDDSDIEVHPNVDKRSFIRAKQNQIHQQRIQRHQEIETLKYSRIIN 59
Coccidioides     -MVLDYSKWDALELSDDSDIEVHPNVDKRSFIRAKQNQIHQQRFQRRQEIATLKYERIIN 59
Candida          -MPIDYSKWDKIEISDDSDVEVHPNVDKQSFIRWKQRDIHEKRMQRNIEIKSILIQLTMY 59
Schiz. pombe     -MAIDYSKWDKLELSDDSDIEVHPNVDKKSFIRWRQRDIHEKRAVRKQKMEDIKGAMAMN 59
Saccharomyces    -MAIDYSKWDKIELSDDSDVEVHPNVDKKSFIKWKQQSIHEQRFKRNQDIKNLETQVDMY 59
                    :*** *. :*:***.*   ***:*. .::: ::.    .      .
```

FIGURE 7: Clustal alignment of the N-terminal region of animal and fungal Cdc37. Sequences from the N-terminal region of Cdc37 from *Homo sapiens* (NP_008996), *Mus musculus* (AAB18761), *Gallus gallus* (AAB91998), *Xenopus laevis* (AAH41715), *Silurana tropicalis* (AL650082), *Tetraodon fluviatilis* (AAG00066), *Danio rerio* (AAH45994), *Drosophila melanogaster* (AAO45184), *Amblyomma variegatum* (BM29091), *Arcoptes scabiei* (BG817795), *Caenorhabditis elegans* (T34050), *Paracoccidioides brasiliensis* (CA581213), *Candida albicans* (Q8X1E6), *Coccidioides immitis* (BF251498), *Metarhizium anisopliae* (BQ142687), *Saccharomyces cerevisiae* (NP_010452), *Magnaporthe grisea* (CD032822), *Neurospora crassa* (EAA27555), and *Schizosaccharomyces pombe* (NP_595752) were aligned using the European Bioinformatics Institute Clustal W program at http://www.ebi.ac.uk/clustalw/#. ( ) - GenBank accession numbers of Cdc37 gene products or ESTs from which open reading frames were translated. (*) - invariant amino acid residues; (:) - conservative amino acid substitutions; (.) - similar amino acid substituions. Symbols above the animal and fungal sequences indicate amino acid similarities between animal or fungal species, respectively. Symbols at the bottom of the figure indicate overall amino acid similarities between both the animal and fungal species.

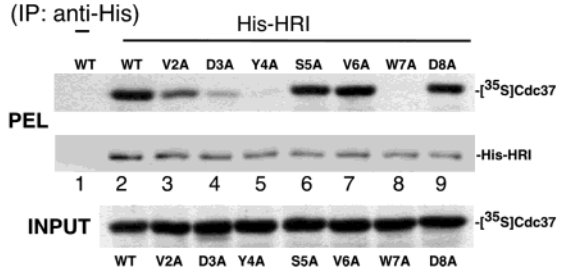

FIGURE 8: HRI-binding activities of the N-terminal point mutants of Cdc37. [^{35}S]-Labeled wild type and the N-terminal point mutants of Cdc37 were synthesized in TnT RRL, and mixed and incubated for 25 min with TnT RRL containing newly synthesized His-tagged-HRI as described in Figure 5 (PEL, lanes 2 to 9). A duplicate TnT RRL reaction synthesizing the wild-type Cdc37 was mixed with a mock TnT RRL mixture lacking His-tagged HRI to serve as the nonspecific binding control (lane 1). Samples were immunoadsorbed with ant-His tag antibody and analyzed as described in Figure 5. His-tagged HRI was detected by Western blot (PEL, lower panel), whereas the coadsorbed [^{35}S]-labeled Cdc37 mutants were analyzed by autoradiography (PEL, upper panel). Equivalent aliquots were taken from each different Cdc37 reaction prior to immunoadsorption to ensure the constructs were generated at comparable levels (INPUT).

To rule out the possibility that the altered functions of Cdc37 mutants V2A, D3A, Y4A, and W7A were caused by gross global disruption of Cdc37 structure versus specific structural or functional roles of these individual residues and their side chains, mild trypsin proteolysis was carried out under native conditions on all of the mutant constructs. Dramatically different proteolysis patterns and/or sensitivities were predicted if these mutants had structures that were grossly compromised. As we have observed previously for the Cdc37/N8aa mutant (*21*), mutation of individual residues 2−8 of Cdc37 induced no changes in either the fragmentation patterns or sensitivities to trypsinolysis relative to wild-type Cdc37 (not shown). This result indicated that the mutations did not induce gross global conformational disruption. However, because of the proximity of the residues to the N-terminus of Cdc37, we cannot rule out the possibility that the mutations induce local structural changes in this region that might be undetectable by native nicking assays.

For full-length Cdc37, Hsp90 is required for Cdc37 to bind protein kinases (*13*, *21*). Thus, the impaired kinase-binding activity of the Cdc37 mutants V2A, D3A, Y4A, and W7A could have resulted from their inability to form complexes with Hsp90. To examine this possibility, these Cdc37 point mutants were synthesized and radiolabeled with [^{35}S]Met in reticulocyte lysate, followed by anti-Hsp90 immunoadsorption of endogenous Hsp90 and autoradiographic assay for coadsorption of radiolabeled Cdc37 gene products. Results indicated that all of the mutants except W7A bound to Hsp90 with efficiencies similar to that the wild type Cdc37. Thus, their Hsp90-binding activities were not detectably affected by these mutations. The interaction of Cdc37/W7A with Hsp90 was decreased by approximately 50% compared to the wild type Cdc37. Similar results were obtained in the reciprocal experiment in which the His-tagged Cdc37 mutants were synthesized in reticulocyte lysate and immunoadsorbed by the anti-His-tag antibody (Figure 9B). Again, the interaction of Cdc37/W7A with Hsp90 was decreased, whereas the other mutants interacted with Hsp90 at essentially the same level compared to the wild-type Cdc37. Therefore, the data presented here further strengthen the hypothesis that the N-terminal amino acids including Val-2, Asp-3, Tyr-4, and Trp-7 are directly involved in the interaction of Cdc37 and its client kinase. Additionally, these data provide novel evidence that segments of this region also modulate Cdc37's interaction with Hsp90.

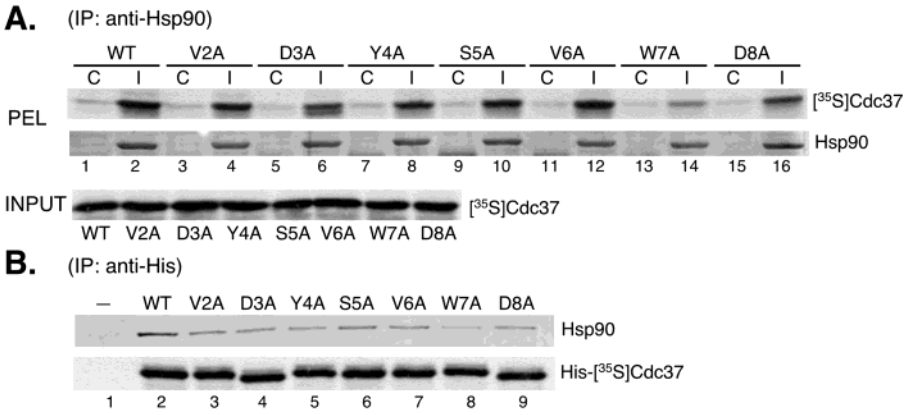

FIGURE 9: Hsp90-binding activities of the N-terminal point mutants of Cdc37. (A) [^{35}S]-Labeled wild type and mutant forms of Cdc37 were synthesized in separate TnT RRL reactions at 30 °C for 30 min, followed by a 10 min chase with 60 μM aurintricarboxylic acid. Samples were immunoadsorbed with the monoclonal anti-Hsp90 antibody 8D3 (even-number lanes) or nonimmune control IgM antibody (odd-number lanes) and analyzed as described in Figure 5. Immunoadsorbed Hsp90 and coadsorbed [^{35}S]-labeled Cdc37 proteins were detected by Western blotting and autoradiography, respectively (PEL). Equivalent aliquots were taken from the Cdc37 translation mixtures prior to immunoadsorption to show that the constructs were synthesized at comparable levels (INPUT). (B) [^{35}S]-Labeled His-tagged wild type and mutant forms of Cdc37 were synthesized in separate TnT RRL as described above. Samples were immunoadsorbed by the anti-His-tag antibody and analyzed as described above. Coadsorbed Hsp90 or [^{35}S]-labeled His-tagged Cdc37 constructs were detected by Western blotting and autoradiography, respectively.

DISCUSSION

In this report, physical data are presented that support a three-domain structure of Cdc37. Our predicted three-domain structure for Cdc37 is strikingly similar to alignment-driven predictions of Scholz et al (*30*). Data presented here indicate that the first 126 amino acids of Cdc37 function as a discrete module that contains the majority of Cdc37's kinase-binding activity. Thus, this segment represents the majority of an authentic domain, but is 37 resides shorter than the previously characterized arbitrary N-terminal Cdc37/ΔC construct (*18*, *21*).

Similarly, Cdc37 residues S127−R283 represent a 157-residue segment whose proteolytic resistance and modular function in Hsp90-binding support its identification as a bona fide domain. Our assignment is larger than the 120-amino acid segment (residues E145−R264) previously predicted from the sequence alignments (*30*). Consistent with our assignment of function, the arbitrary N-terminal truncation Cdc37/ΔN (amino acids M164−V378) is also sufficient to bind Hsp90. While these observations predict that major Hsp90-binding motifs lie between residues M164 and R264, we favor defining the central Hsp90-binding domain as amino acid residues S127−R283 on the basis of this segment's high resistance to proteolytic nicking, a criterion that has not been previously applied to definitions of Cdc37's domain architecture. Consistent with this assignment, limited proteolysis of Cdc37 by chymotrypsin generates a strikingly similar pattern of fragments to that generated by trypsin (Shao and Matts, unpublished observations).

Hsp90 and Cdc37 are known to be functional partners that utilize Hsp90's nucleotide-mediated conformational switching to regulate binding to Hsp90-dependent kinases. Results presented here illuminate the Cdc37 motifs underlying this partnership and suggest a novel mechanistic model.

Three observations indicate that within the context of the Hsp90−Cdc37 partnership, the C-terminal half of the middle domain of Cdc37 ("D2b," residues M164 to E282) contains the major Hsp90-binding motifs that sense Hsp90's conformation. (i) Cdc37 constructs that lacked these residues (D1, D3, and Cdc37/ΔC) did not bind Hsp90 [(*14*, *18*, *21*) and Figure 3]. (ii) Cdc37 constructs that contained these residues (D12, D2, D23, and Cdc37/ΔN) bound Hsp90. And most significantly, (iii) the Cdc37 gene product that contained D2b, but lacked the N-terminal half of the middle domain, Cdc37/ΔN was a potent *sensor* of Hsp90's default, geldanamycin-induced, and novobiocin-induced conformations (Figures 3 and 4), and also bound to Hsp90−kinase in the presence of geldanamycin (Figure 6). Furthermore, the novobiocin-bound conformation of Hsp90 was different from Hsp90's molybdate-bound conformation, as in the presence of molybdate anti-His antibodies immunoadsorbed His-tagged Cdc37/ΔN and coadsorbed Hsp90 at levels nearly equivalent to those immunoadsorbed in the presence of geldanamycin (Figure 4C).

However, our data also suggest that the other half of this domain, namely, residues S127 to G163 (D2a), *represses* D2b's ability to readily recognize and accommodate different conformations of Hsp90. The argument that the function of D2b is modulated by upstream segments from D2a, derives from the observation that Cdc37 gene products containing D2a in conjunction with the D2b "sensor" motif, (D2, D12, and D23) have essentially wild-type behavior. While the D2 and D23 constructs displayed somewhat suppressed Hsp90 binding activity in the presence of geldanamycin, in general constructs containing the complete middle domain of Cdc37 (D2a+D2b) no longer demonstrated the very dramatic ability to sense and respond to Hsp90 conformation that is exhibited by the Cdc37/ΔN construct, which lacks D2a (Figure 3). Thus, D2a may function as a repressor of D2b's ability to sense Hsp90 conformation.

While the results from limited proteolysis of Cdc37 support the notion that amino acids S127−G163 are part of domain D2, D2a also impacted the kinase-binding activity of D1. D1 binds kinase, but does so in a regulated (geldanamycin-sensitive) manner. However, the Cdc37/ΔC construct (D1+D2a) has an enhanced kinase-binding capacity that is dysregulated, as it is unaffected by geldanamycin [(*14*, *18*, *21*) and Figure 6]. Thus, D2a has the apparent ability to

modulate both the Hsp90 and kinase-binding activities of Cdc37.

These conclusions invite a speculative, but heuristic, model for the Cdc37−Hsp90 partnership (Figure 10). In this model, the default interaction of D2a with D2b dampens the ability of D2b to interact with Hsp90−kinase, which also results in the restraint of the kinase-binding potential of D1 (Figure 10A, step 1). Upon interaction of Cdc37 with Hsp90−kinase complexes, D2a functions to sense and communicate the binding of kinase client at D1 to D2 (Figure 10A, steps 1 to 2): D2a participates in and is responsive to client binding (see Figures 5 and 6). Thus, client binding at D1 relieves D2a's repression of D2b's interactions with Hsp90−kinase complexes. At the same time, D2b may interpret cues from Hsp90−kinase complexes to communicate the coincident binding of nucleotide and/or client at sites elsewhere within the Hsp90 chaperone heterocomplex (Figure 10A, step 2). This communication would be passed from D2b to D2a and hence to D1, ultimately triggering nucleotide-modulated conformational switching of Hsp90, resulting in the establishment of the salt-stabile, high-affinity interactions typical of Hsp90−Cdc37−kinase heterocomplexes (Figure 10A, step 3). These steps would also include ATP-induced binding of the co-chaperone p23, ATP-induced N-terminal domain clamping, and nucleotide hydrolysis (*40*−*43*). Thus, the model suggests that the Hsp90−Cdc37 heterocomplex engages in an elegant conformational conversation, in which multiple binding events are communicated via a nucleotide-mediated process with hallmarks of allosterism, and accounts for the observation that C-terminal regions of Hsp90 are required to "trap" nucleotide bound to the N-terminal domain of Hsp90 (*43*). This model is also consistent with our recent findings that conformational switching of Hsp90 is triggered by multiple discrete segments of its kinase clients that interact with Cdc37 and Hsp90 (Scroggins et al., submitted).

In regard to this model, the binding of client substrate to Hsp90 presumably requires that Hsp90 be present in its "open" or "relaxed" conformation (*37*, *40*, *41*, *44*−*47*). It is currently unclear whether this substrate-binding competent conformation of Hsp90 represents the ADP-bound (Figure 10A, step 4) or nucleotide-free conformation(s) of Hsp90 (step 5), or ATP-bound Hsp90 (step 1) in association with a co-chaperone component that inhibits N-terminal domain "clamping". The model presented in Figure 10 is of necessity incomplete because it is not known what events induce the dissociation of phosphate and client substrate (step 4), what stimulates nucleotide exchange within the N-terminal ATP binding domain of Hsp90 (step 5), and what stimulates the dissociation of Cdc37 (*13*, *48*). These events are undoubtedly regulated in part via the association and dissociation of client, other co-chaperone partners, and the binding of ATP to the C-terminal ATP (novobiocin) binding site of Hsp90 (*37*−*39*, *41*, *42*, *44*, *47*, *49*−*51*).

With respect to the model proposed here, Cdc37 is known to form a complex with geldanamycin-bound Hsp90, which adopts an opened conformation for substrate binding (*13*, *21*, *44*). Cdc37 has no effect on the binding of geldanamycin to the N-terminal ATP-binding site of Hsp90 (*44*), suggesting that "communication" between the N-terminal nucleotide binding site and the Cdc37 binding site within the C-terminal region of Hsp90 has been disrupted. As a consequence of the disruption of this interdomain communication, we

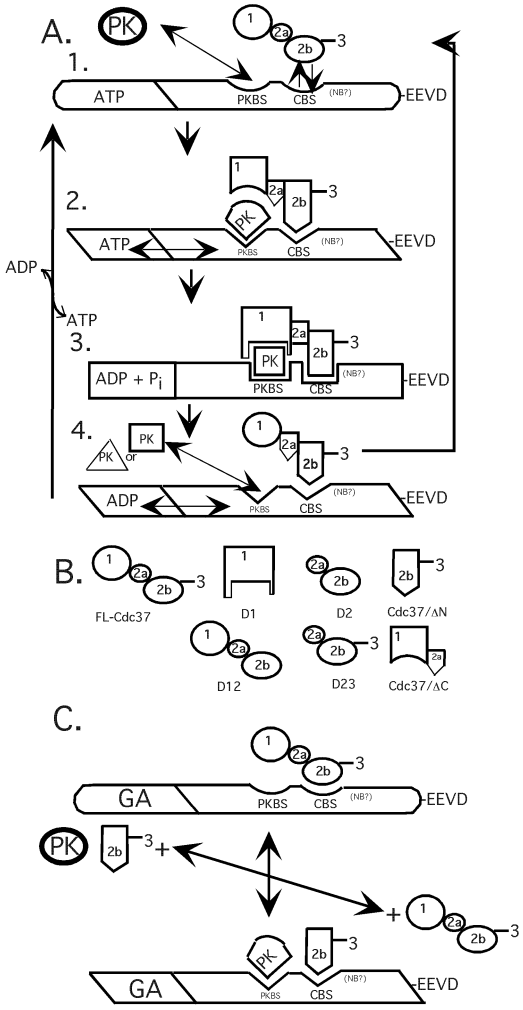

FIGURE 10: Model for domain interactions that modulate the kinase-binding and Hsp90-binding activities of Cdc37. (A) Step 1: Reversible interactions of newly syntheisized protein kinase (PK) and Cdc37 with the protein kinase binding site (PKBS) and Cdc37 binding site (CBS) on ATP-bound Hsp90. Step 2: Coincident binding of Cdc37 to kinase and Hsp90 alter interactions between the D1, D2a and D2b subdomains of Cdc37. These changes alter the interaction of kinase with Hsp90, Hsp90 with Cdc37, and Cdc37 with kinase (implied by shape changes in the cartoon). The induced conformational changes are sense through allosteric interactions between the N-terminal ATP binding site of Hsp90 and its C-terminal domains (two-way arrow). Step 3: Changes in the conformations of Hsp90 and Cdc37 induced by the interactions summarized in step 2 cause nucleotide modulated conformational switching, ATP hydrolysis, and N-terminal domain "clamping", resulting in the establishment of salt-stabile high affinity interactions between Hsp90, Cdc37, and kinase. Step 4: Completion of the ATP-driven reaction cycle of Hsp90 requires phosphate dissociation, and release of client kinase (triangle = folded kinase; square = partially folded immature kinase), and (step 5) Cdc37 release and the exchange of ADP for ATP. Displacement of phosphate by molybdate may explain the ability of molybdate to inhibit Hsp90's reaction cycle and stabilize Hsp90−client complexes. As noted in the text of the paper, the exact sequence of these events from step 3 through steps 4 and 5 and the mechanisms that induce and regulate these events are not clearly understood. (B) Cartoons used to imply alterations in domain conformations induced by the presence or absence of subdomains of Cdc37 and their interactions with Hsp90 and kinase. (C) Conformations of geldanamycin-bound Hsp90 that are proposed to explain the mutually exclusive versus coincident binding of specific Cdc37 constructs with Hsp90 and Hsp90−kinase complexes.

propose that the geldanamycin-bound form of Hsp90 is in an intermediate conformation, between Hsp90's ADP- and ATP-bound forms. In this state, the kinase-binding and Cdc37-binding sites of Hsp90 may be capable of undergoing conformational changes independent of nucleotide-modulated conformational switching. Thus, the binding of substrate to geldanamycin-bound Hsp90 may induce a conformational change in the Cdc37 binding site of Hsp90 (Figure 10A, steps 1 to 2, and C). In the absence of nucleotide modulated conformational switching of Hsp90, the D2a subdomain of Cdc37 suppresses the ability of D2b to alter its conformation and constructs of Cdc37 containing D2a (Cdc37, D12, D2, and D23) dissociate from the Cdc37 binding site. Alternately, in the presence of geldanamycin the binding of Cdc37 constructs containing both D2a and 2b prevent conformational changes from occurring that are required for the formation of stable complexes between Hsp90 and kinase. Thus, the binding of these constructs of Cdc37 to Hsp90 and the binding of kinase to Hsp90 are mutually exclusive and stable complexes of these Cdc37 constructs with Hsp90−kinase complexes cannot form in the presence of geldanamycin.

In the absence of D2a, the conformation of D2b is no longer constrained (Figure 10B), and it readily binds to the geldanamycin-bound form of Hsp90, in the presence or absence of bound kinase (Figure 10C). In addition, interaction of either kinase or D2b with Hsp90 may induce conformational changes within Hsp90 that favor the binding of the other molecule. However, in the absence of geldanamycin the conformation of Hsp90 favors the binding of the default conformation of Cdc37 adopted via the interaction of D2a with D2b (Figure 10A, step 1, and C). Reduction of the binding of Cdc37/ΔN to Hsp90 in the absence of geldanamycin may be due to restraint of nucleotide-modulated conformational switching of the Cdc37-binding site on Hsp90 in the absence of client kinase (Figure 10A, steps 1 to 2) or the ratio of Hsp90 present at step 4 versus step 1 of its ATP-driven reaction cycle.

In its geldanamycin-bound conformation, the client binding pocket of Hsp90 is open and substrate is free to reversibly bind and dissociate from Hsp90 (*13*, *21*, *37*, *41*, *43*−*47*, *52*). In its default conformation, the kinase-binding activity of the D1 domain of Cdc37 is constrained through its interactions with the D2a and D2b subdomains, such that Cdc37 constructs that contain D1, and the complete D2 domain cannot bind kinase in the absence of Hsp90 and in the absence of nucleotide-modulated conformational switching of Hsp90 (this paper and refs *13* and *21*). Our model predicts that in the absence of subdomain D2b constraining the interaction of D2a with D1 (Figure 10B), the conformation of the kinase-binding domain of the Cdc37/ΔC construct (D1+D2a) can directly bind newly synthesized kinase or it can bind kinase as it reversibly dissociates from Hsp90 in the presence of geldanamycin. The model further predicts that the kinase-binding conformation of D1 in the absence of D2a interacts with kinase whose conformation has been altered by nucleotide-modulated conformational switching of Hsp90. We have previously demonstrated using pulse-chase analyzes that Cdc37 dissociates from newly synthesized HRI during reiterative cycles of Hsp90 action required for the maturation of HRI (*13*, *48*). Thus, the presence of geldanamycin would inhibit the ATP-driven reaction cycle of Hsp90, the release of immature kinase from Hsp90 after completion of this cycle, and the subsequent binding of kinase by the Cdc37 D1 construct.

Shifting our attention to specific amino acid residues of Cdc37, our site-directed mutagenesis studies indicate that amino acid residues at the N-terminus of Cdc37 are involved in kinase binding. Four residues at the N-terminus of Cdc37 are critical for its interaction with client kinase: V2, D3, Y4, and W7 (Figure 8). Consistent with the effects of these mutations, our previous characterizations demonstrated that replacing the first eight amino acids of Cdc37 with an unrelated sequence completely abolishes its ability to bind HRI (*21*). Furthermore, sequence alignment of Cdc37 homologues from different species in two kingdoms ranging from yeast to human reveals that the first 30 or so amino acids are the most conserved region of the whole protein, and three out of the four residues (namely, D3, Y4, and W7) now identified as being critical for kinase binding are absolutely invariant, while the fourth amino residue contains the conservative substitution of V to I/L.

In contrast, mutation of the conserved S5 residue, and of the unconserved residues V6 and D8, did not affect binding of Cdc37 to HRI. Thus, these residues do not seem to play a role in kinase binding or are not critical for maintaining the integrity of Cdc37's kinase-binding site. Thus, our data strongly suggest an evolutionarily conserved function for these N-terminal amino acid residues in the recognition and binding of client proteins kinases by Cdc37.

Mutations at Cdc37's N-terminus may alter its kinase-binding potential by at least three different mechanisms. (i) The mutations may disrupt the local structure(s) that govern kinase-binding mediated by other amino acid residues within the N-terminal domain of Cdc37. (ii) These residues may participate directly in the intermolecular interactions between Cdc37 and its client kinases. (iii) These residues may represent a regulatory element that modulates Cdc37's kinase-binding activity in response to Hsp90 nucleotide-dependent conformational switching. The third possibility is supported by the observation that one of the mutations characterized, namely, W7A, compromised both Cdc37's ability to bind HRI and its ability to interact with Hsp90. This impact on Hsp90 interaction, which can clearly be segregated from its impact on kinase-binding per se, indicates the potential for such a role for the N-terminal segments of Cdc37, and implies that the impacts of the other mutations may actually result from compromised communications with Hsp90 rather than from alterations in Cdc37's raw kinase-binding potential. This hypothesis is further supported by the documented dynamic nature of the Hsp90−Cdc37 partnership (*13*), and by our identification here of a similar communication motif elsewhere on Cdc37. This hypothesis is also intriguing due to our recent finding that phosphorylation of Cdc37 on Ser13 is required for the kinase-binding activity of Cdc37 and for the ability of Cdc37 the coordinate kinase binding with nucleotide-mediated conformational switching of Hsp90 (*48*). Further investigations into the role(s) of these motifs and their mechanisms of action are ongoing.

In summary, data presented in this report reveal the authentic domain structure of Cdc37. Detailed dissection of this structure in conjunction with biochemical characterizations demonstrate that the Hsp90−Cdc37 partnership is

mediated by two discrete regions within the middle domain of Cdc37, with the downstream motifs (D2b) functioning to sense and accommodate at least three nucleotide-regulated Hsp90 conformations, and with the upstream region (D2a) functioning to repress such sensing and to modulate or communicate D1's binding of kinase.

ACKNOWLEDGMENT

The authors would like to thank Dr. Douglas Melton (Harvard University) for generously providing the pSP64T plasmid DNA. Geldanamycin was provided by the Drug Synthesis and Chemistry Branch, Developmental Therapeutics Program, Division of Cancer Treatment, National Cancer Institute, NIH. We would like to thank the Sarkey's Biotechnology Research Laboratory (OSU) for oligonucleotide synthesis, DNA sequencing, and MALDI-TOF MS analysis, and the Protein Core Facility at the University of Oklahoma Health Sciences Center for peptide sequencing. Polyclonal mouse ascites antibodies against Hsp90 were prepared by the Oklahoma State University Hybridoma Center for the Agricultural and Biological Sciences.

REFERENCES

1. Pearl, L. H., and Prodromou, C. (2002) *Adv. Prot. Chem. 59*, 157−185.
2. Picard, D. (2002) *Cell Mol. Life Sci. 59*, 1640−8.
3. Richter, K., and Buchner, J. (2001) *J. Cell. Physiol. 188*, 281−90.
4. Dai, K., Kobayashi, R., and Beach, D. (1996) *J. Biol. Chem. 271*, 22030−22034.
5. Stepanova, L., Leng, X., Parker, S. B., and Harper, J. W. (1996) *Genes Dev. 10*, 1491−1502.
6. Lamphere, L., Fiore, F., Xu, X., Brizuela, L., Keezer, S., Sardet, C., Draetta, G. F., and Gyuris, J. (1997) *Oncogene 14*, 1999−2004.
7. Mahony, D., Parry, D. A., and Lees, E. (1998) *Oncogene 16*, 603−11.
8. O'Keeffe, B., Fong, Y., Chen, D., Zhou, S., and Zhou, Q. (2000) *J. Biol. Chem. 275*, 279−287.
9. Estable, M. C., Naghavi, M. H., Kato, H., Xiao, H., Qin, J., Vahlne, A., and Roeder, R. G. (2002) *J. Biomed. Sci. 9*, 234−45.
10. Brugge, J. S. (1986) *Curr. Top. Microbiol. Immunol. 123*, 1−22.
11. Dey, B., Lightbody, J. J., and Boschelli, F. (1996) *Mol. Biol. Cell 7*, 1405−1417.
12. Perdew, G. H., Wiegand, H., Vanden Heuvel, J. P., Mitchell, C., and Singh, S. S. (1997) *Biochemistry 36*, 3600−3607.
13. Hartson, S. D., Irwin, A. D., Shao, J., Scroggins, B. T., Volk, L., Huang, W., and Matts, R. L. (2000) *Biochemistry 39*, 7631−7644.
14. Scholz, G., Hartson, S. D., Cartedge, K., Hall, N., Shao, J., Dunn, A. R., and Matts, R. L. (2000) *Mol. Cell. Biol. 20*, 6984−6995.
15. Glover, C. V. (1998) *Prog. Nucleic Acid Res. Mol. Biol. 59*, 95−133.
16. Kimura, Y., Rutherford, S. L., Miyata, Y., Yahara, I., Freeman, B. C., Yue, L., Morimoto, R. L., and Lindquist, S. (1997) *Genes Dev. 11*, 1775−1785.
17. Bandhakavi, S., McCann, R. O., Hanna, D. E., and Glover, C. V. (2003) *J. Biol. Chem. 278*, 2829−36.
18. Grammatikakis, N., Lin, J.-H., Grammatikakis, A., Tsichlis, P. N., and Cochran, B. H. (1999) *Mol. Cell. Biol. 19*, 1661−1672.
19. Tzivion, G., Luo, Z., and Avruch, J. (1998) *Nature 394*, 88−92.
20. Miyata, Y., Ikawa, Y., Shibuya, M., and Nishida, E. (2001) *J. Biol. Chem. 276*, 21841−8.
21. Shao, J., Gramatikakis, N., Scroggins, B., Uma, S., Huang, W., Chen, J.-J., Hartson, S. D., and Matts, R. L. (2001) *J. Biol. Chem. 276*, 206−214.
22. Donze, O., Abbas-Terki, T., and Picard, D. (2001) *EMBO J. 20*, 3771−80.
23. Donze, O., and Picard, D. (1999) *Mol. Cell Biol. 19*, 8422−32.
24. Chen, G., Cao, P., and Goeddel, D. V. (2002) *Mol. Cell 9*, 401−10.
25. Basso, A. D., Solit, D. B., Chiosis, G., Giri, B., Tsichlis, P., and Rosen, N. (2002) *J. Biol. Chem. 277*, 39858−66.
26. Fliss, A. E., Fang, Y., Boschelli, F., and Caplan, A. J. (1997) *Mol. Biol. Cell 8*, 2501−2509.
27. Rao, J., Lee, P., Benzeno, S., Cardozo, C., Albertus, J., Robins, D. M., and Caplan, A. J. (2001) *J. Biol. Chem. 276*, 5814−20.
28. Wang, X., Grammatikakis, N., and Hu, J. (2002) *J. Biol. Chem. 277*, 24361−7.
29. Lee, P., Rao, J., Fliss, A., Yang, E., Garrett, S., and Caplan, A. J. (2002) *J. Cell Biol. 159*, 1051−9.
30. Scholz, G. M., Cartledge, K., and Hall, N. E. (2001) *J. Biol. Chem. 276*, 30971−9.
31. Hartson, S. D., and Matts, R. L. (1994) *Biochemistry 33*, 8912−8920.
32. Uma, S., Hartson, S. D., Chen, J.-J., and Matts, R. L. (1997) *J. Biol. Chem. 272*, 11648−11656.
33. Uma, S., Matts, R. L., Guo, Y., White, S., and Chen, J.-J. (2000) *Eur. J. Biochem. 267*, 498−506.
34. Kreig, P. A., and Melton, D. A. (1984) *Nuc. Acids Res. 12*, 7057−7070.
35. Perdew, G. H. (1988) *J. Biol. Chem. 263*, 13802−13805.
36. Johnson, J. L., and Toft, D. O. (1995) *Mol. Endocrinol. 9*, 670−678.
37. Kanelakis, K. C., Shewach, D. S., and Pratt, W. B. (2002) *J. Biol. Chem. 277*, 33698−703.
38. Marcu, M. G., Chadli, A., Bouhouche, I., Catelli, M., and Neckers, L. M. (2000) *J. Biol. Chem. 275*, 37181−6.
39. Soti, C., Racz, A., and Csermely, P. (2001) *J. Biol. Chem. 277*, 7066−75.
40. Wegele, H., Muschler, P., Bunck, M., Reinstein, J., and Buchner, J. (2003) *J. Biol. Chem*.
41. Prodromou, C., Panaretou, B., Chohan, S., Siligardi, G., O'Brien, R., Ladbury, J. E., Roe, S. M., Piper, P. W., and Pearl, L. H. (2000) *EMBO J. 19*, 4383−92.
42. Sullivan, W. P., Owen, B. A., and Toft, D. O. (2002) *J. Biol. Chem. 277*, 45942−8.
43. Weikl, T., Muschler, P., Richter, K., Veit, T., Reinstein, J., and Buchner, J. (2000) *J. Mol. Biol. 303*, 583−92.
44. Siligardi, G., Panaretou, B., Meyer, P., Singh, S., Woolfson, D. N., Piper, P. W., Pearl, L. H., and Prodromou, C. (2002) *J. Biol. Chem. 277*, 20151−9.
45. Sullivan, W., Stensgard, B., Caucutt, G., Bartha, B., McMahon, N., Alnemri, E. S., Litwack, G., and Toft, D. (1997) *J. Biol. Chem. 272*, 8007−8012.
46. Richter, K., Muschler, P., Hainzl, O., and Buchner, J. (2001) *J. Biol. Chem. 276*, 33689−96.
47. Panaretou, B., Prodromou, C., Roe, S. M., O'Brien, R., Ladbury, J. E., Piper, P. W., and Pearl, L. H. (1998) *EMBO J. 17*, 4829−4836.
48. Shao, J., Prince, T., Hartson, S. D., and Matts, R. L. (2003) *J. Biol. Chem*. 278, 38117−20.
49. McLaughlin, S. H., Smith, H. W., and Jackson, S. E. (2002) *J. Mol. Biol. 315*, 787−98.
50. Prodromou, C., Siligardi, G., O'Brien, R., Woolfson, D. N., Regan, L., Panaretou, B., Ladbury, J. E., Piper, P. W., and Pearl, L. H. (1999) *EMBO J. 18*, 754−762.
51. Panaretou, B., Siligardi, G., Meyer, P., Maloney, A., Sullivan, J. K., Singh, S., Millson, S. H., Clarke, P. A., Naaby-Hansen, S., Stein, R., Cramer, R., Mollapour, M., Workman, P., Piper, P. W., Pearl, L. H., and Prodromou, C. (2002) *Mol. Cell 10*, 1307−18.
52. Hartson, S. D., Thulasiraman, V., Huang, W., Whitesell, L., and Matts, R. L. (1999) *Biochemistry 38*, 3837−3849.

BI035138J